ISSN 0036-0244, Russian Journal of Physical Chemistry A, 2019, Vol. 93, No. 2, pp. 333–337. © Pleiades Publishing, Ltd., 2019.
Russian Text © S.B. Yarusova, P.S. Gordienko, A.E. Panasenko, N.N. Barinov, L.A. Zemnukhova, 2019, published in Zhurnal Fizicheskoi Khimii, 2019, Vol. 93, No. 2, pp. 278–283.

PHYSICAL CHEMISTRY
OF SURFACE PHENOMENA

Sorption Properties of Sodium and Potassium Aluminosilicates from Alkaline Hydrolyzates of Rice Straw

S. B. Yarusova[a,b], P. S. Gordienko[a], A. E. Panasenko[a,c,*], N. N. Barinov[d], and L. A. Zemnukhova[a,c]
[a] *Institute of Chemistry, Far Eastern Branch, Russian Academy of Sciences, Vladivostok, 690022 Russia*
[b] *Vladivostok State University of Economics and Service, Vladivostok, 690041 Russia*
[c] *Far Eastern Federal University, Vladivostok, 690950 Russia*
[d] *Far East Geological Institute, Far Eastern Branch, Russian Academy of Sciences, Vladivostok, 690022 Russia*
**e-mail: panasenko@ich.dvo.ru*

Received February 28, 2018

Abstract—Sodium and potassium aluminosilicates samples are synthesized from solutions formed via the alkaline hydrolysis of rice straw. The fabricated samples are characterized by means of X-ray diffraction analysis and IR-spectroscopy, and their elemental composition, particle morphology, specific surface area, and thermal properties are determined. The sorption properties of the synthesized aluminosilicates with respect to Cs^+ ions are investigated under static conditions. Kinetic curves and sorption isotherms are provided and a sorption kinetic model is described.

Keywords: aluminosilicates, X-ray diffraction analysis, IR-spectroscopy, sorption kinetic model
DOI: 10.1134/S003602441902033X

INTRODUCTION

The complex processing of renewable vegetable raw materials is a crucial factor in increasing the efficiency of the agricultural industry and producing a wide range of valuable materials for diverse industrial fields.

Stocks of renewable sources of vegetable raw materials, including byproducts of annual grain crops (straw and grain coating, also known as chaff, husk, or peeling) are estimated at millions of tons each year in Russia. However, the utilization ratio of these raw materials is extremely low. Annual plant wastes are most commonly used to produce coarse low-value feed for ruminants, as nesting or packaging material, or as fuel. At the same time, the vegetable biomass constantly renewable due to photosynthesis, the volume of which exceeds the total production of coal, oil, and gas, represents promising raw materials for producing a wide range of valuable substances and materials. Yearly reproducibility along with low cost are the main advantages of these raw materials. Complete and accurate data on the chemical composition of substances contained in a plant, and their properties and optimum conditions for synthesis, are required in order to develop efficient processing technologies for vegetable raw materials, and they are often not available. This applies to rice straw in particular. There are fewer examples [1, 2] of using rice straw in chemical industry than using husk (grain coating). This is probably due to the bulk of straw stock being traditionally used in the agricultural sector itself, and a very small amount being used in the hydrolysis industry [3]. There is only one published work on processing grain crop straw [4] that includes information on rice straw.

The rice straw of the Primorye region varieties is from 4 to 16% of silica [5], so it can be used as raw materials to produce amorphous silica, the output and properties of which depend on the variety of rice and the means of processing (acidic or alkaline hydrolysis).

It is worth noting that the properties of amorphous silica produced from rice straw remain poorly studied. The data obtained in [6] on the sorption of Mn(II) ions from aqueous solutions by silica samples produced from rice straw and husks using the same technology had different parameters of the samples' surfaces.

Both acidic and alkaline waste waters (hydrolizates, extracts) can form upon processing byproducts of annual crops, depending on the scheme of manufacturing the end product, which must be processed according to current regulatory requirements on environmental protection [7, 8]. Alkaline hydrolyzates can be processed by different means with the extraction of such valuable components as polysaccharides [9], corrosion inhibitors [10], and amorphous silica [11]. However, there are currently no ways of extracting valuable components from the waste of rice production that can be used in industry.

As was demonstrated at the Institute of Chemistry, Far Eastern Branch, Russian Academy of Sciences [12], fabricating nanostructured aluminosilicates of alkali metals is one promising way of utilizing the rice straw hydrolyzates. This work was a followup of earlier studies on synthesizing nanostructured aluminosilicates and their subsequent use as sorbents for removing Cs^+ ions from aqueous solutions, including those of complex salt composition [13–16].

Note that a great many works published worldwide have been dedicated to the hydrothermal synthesis of zeolites, where the rice husk ashes are used fully or partially as a silicon-containing component [17–21]. There have been far fewer works focused on the properties of aluminosilicates from rice straw [22, 23].

The aim of this work was to investigate the sorption properties of sodium and potassium alumina silicates synthesized from alkaline hydrolizates of rice straw.

EXPERIMENTAL

Two samples of rice straw (RS) of the Darii-23 and Lugovoi varieties were collected in the town of Timiryazevskii in 2010. The straw was ground into sections 10–50 mm long, washed with water, and dried in air. Each sample of the material was then treated with 1 M solution of potassium hydroxide (for the Darii-23 variety) or sodium hydroxide (for the Lugovoi variety) at 90°C for 1 h. The straw residue (which could subsequently be used as a raw material for the production of cellulose materials) was then separated from the solution, to which a saturated solution of $Al_2(SO_4)_3 \cdot 18H_2O$ was added to reach pH 7. The formed precipitate was filtered, washed with water until complete removal of SO_4^{2-} ions, and dried in air at 60°C (the samples were marked as I and II, respectively).

The X-ray diffraction patterns were recorded using a Bruker D8 Advance diffractometer (Germany) with CuK_α irradiation. Elemental analysis was performed via energy-dispersive X-ray fluorescence spectroscopy on a Shimadzu EDX 800 HS spectrometer (Japan). The analysis was performed using spectrometer software that ignored light elements. The relative error did not exceed ±2%. The IR absorption spectra of the samples were recorded in the range of 400–4000 cm^{-1} using a Spectrum-1000 Fourier transform spectrometer (PerkinElmer, USA). The samples' morphology was investigated using an EV0-50XVP scanning electron microscope (SEM) equipped with an INCA Energy-350 X-ray energy-dispersive system (LEO, Germany). The samples' specific surface area was determined by means of low-temperature nitrogen adsorption using a Sorbtometr-M unit (Russia).

Sorption experiments were performed under static conditions at 20°C and a liquid : solid phase ratio of 1 : 40 from aqueous solutions of cesium carbonate with varied initial concentrations of Cs^+ ions in the range of 0.1 to 26.6 mmol L^{-1} with constant stirring in a magnetic stirrer for 3 h. As a control experiment, a sample of sorbent was placed into a tube filled with distilled water and stirred in parallel with the investigated sample. The solutions were then separated from the sorbent by filtering (blue ribbon paper filter), and the concentrations of Cs^+, K^+, and Na^+ ions were determined.

To obtain the sorption kinetic curves under similar conditions, each sample (I and II) was placed into a series of test tubes filled with Cs_2CO_3 aqueous solution of initial Cs^+ concentrations of 7.2 mmol L^{-1} and stirred from 1 to 60 min.

The concentrations of cesium, potassium, and sodium ions were determined via atomic absorption spectrometry (AAS) using a Solaar M6 two-beam spectrometer (Thermo Scientific, USA) on analytical lines of 852.1, 766.5, and 586.6 nm, respectively. The limit of cesium ion detection in aqueous solutions was 0.01 μg mL^{-1}; that of potassium, up to 0.002 μg mL^{-1}; that of sodium, up to 0.0002 μg mL^{-1}. The relative error in detecting these ions via AAS was 15%.

The sorption capacity (A_s, mmol g^{-1}) of the samples was calculated using the formula

$$A_s = \frac{(C_{init} - C_{eq})}{m}V,$$

where C_{init} is the initial concentration of Cs^+ in the solution, mmol L^{-1}; C_{eq} is the equilibrium concentration of Cs^+ ions in the solution, mmol L^{-1}; V is the solution volume, L; and m is the sorbent's weight, g.

The extraction ratio of Cs^+ ions (α, %) was calculated using the formula

$$\alpha = \frac{(C_{init} - C_{eq})}{C_{init}} \times 100\%.$$

The kinetic data on the sorption of metal ions was analyzed using kinetic models of pseudo-first and pseudo-second orders [24, 25]. The kinetic equation of the pseudo-first order (the Lagergren equation) can be written as

$$\frac{dA_t}{dt} = k_1(A_{eq} - A_t),$$

where k_1 is the sorption rate constant of the pseudo-first order model; A_{eq}, A_t are the sorption capacities at the equilibrium state and at time t, respectively.

The equation take a linear integral form under the initial conditions ($A_t = 0$ at $t = 0$ and $A_t = A_t$ at the time $t = t$):

$$\log(A_{eq} - A_t) = \log A_{eq} - \frac{k_1}{2.303}t.$$

The pseudo-second order kinetic model is expressed by the equation

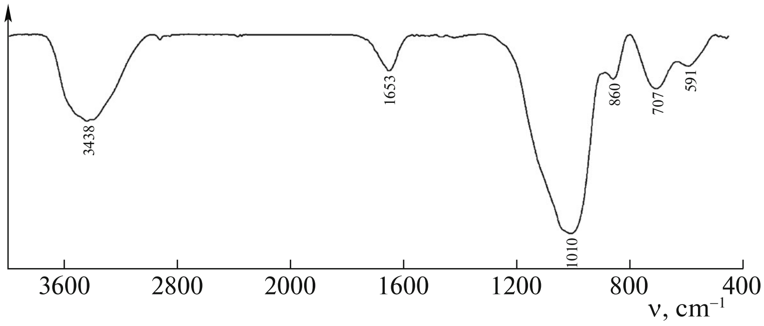

Fig. 1. IR absorption spectrum of potassium aluminosilicate from rice straw (sample II).

$$\frac{dA_t}{dt} = k_2(A_{eq} - A_t)^2,$$

where k_2 is the sorption rate constant of the pseudo-second order model. This expression can be transformed into

$$\frac{t}{A_t} = \frac{1}{k_2 A_{eq}^2} + \frac{1}{A_{eq}} t.$$

RESULTS AND DISCUSSION

Characterizing the Synthesized Potassium and Sodium Aluminosilicates

The synthesized samples were apparently X-ray amorphous, according to the X-ray analysis data. The X-ray diffraction patterns showed halos with maxima corresponding to an interplanar distance of 3.20 Å for sample I and 3.22 Å for sample II.

The X-ray images of both samples after annealing at 1000°C for 1 h showed amorphous peaks in the range of 15°–35°. Peaks related to the aluminosilicate $NaAlSiO_4$ of a triclinic modification (PDF-2, 00-033-1203) with unit cell parameters (a) 5.03470, (b) 5.08220, (c) 16.91000, and $\alpha = 99.000°$, $\beta = 81.500°$, $\gamma = 119.090°$ were recorded against the amorphous peak of sample II. Sample I remained X-ray amorphous, and the interplanar distance grew to 3.41 Å.

Quantitative determination of the elemental compositions of the synthesized samples revealed the following elements in them (wt %). Sample I: K, 16.7; Al, 10.6; Si, 19.2. Sample II: Si, 19.6; Al, 13.5; Na, 11.2. These compositions corresponded to molar ratios of main elements M : Al : Si : 1.09 : 1 : 1.74 for sample I, and 0.97 : 1 : 1.39 for sample II.

The yield of potassium and sodium aluminosilicates from rice straw hydrolizates relative to the initial straw weight was 9.7% for sample I and 14.5% for sample II. The weight loss for the investigated samples upon annealing was 26–27%.

The IR spectra of the synthesized aluminosilicates (Fig. 1) showed intensive absorption bands in the range of asymmetric stretching vibrations of siloxane bonds (Si–O–Si) (1018 cm^{-1} for sample I and 1010 cm^{-1} for sample II), and a specific band of Al–O–Si bonds at ~860 cm^{-1}. Low-frequency bands in the range of 450–600 cm^{-1} were attributed to the bending vibrations of Si–O–Si and Al–O–Si bonds. The bands around 3438 cm^{-1} ν(O–H) and 1653 cm^{-1} δ(O–H) indicated the presence of bound water in the sample [26].

According to the scanning electron microscopy data (Fig. 2), the samples consisted primarily of agglomerates of particles with developed surface relief, and there were some large particles with plate-like shapes and sizes of up to 500 μm. Smaller agglomerates of a complex shape with sizes of several to several dozen μm were observed as well. The agglomerates' surfaces consisted of variously shaped particles, some of which were denser with smooth surfaces and some were loose particles that formed assemblies of smaller grains (up to 1 μm). Multiple pores with sizes of up to several dozen μm were detected visually on the surfaces of the large plate-shaped particles.

The specific surface area determined via BET was 84.8 $m^2 g^{-1}$ for sample I and to 32.7 $m^2 g^{-1}$ for sample II.

Sorption of Cesium Ions

The sorption isotherms (Fig. 3) were built based on the obtained experimental data on the sorption of Cs^+ ions by the investigated sorbents. As seen from the Fig. 3, the sorption capacity of the sample II towards cesium ions appeared to be higher than in case of the sample I.

To estimate the sorption properties of samples I and II, the obtained isotherms were analyzed in regard to the corresponding coordinates of the Langmuir equation:

$$\frac{C_{eq}}{A_s} = \frac{1}{A_{max} k} + \frac{C_{eq}}{A_{max}},$$

where C_{eq} is the equilibrium concentration of Cs^+ ions in the solution, A_{max} is the maximum sorption capacity, and k is the Langmuir constant. The parameters

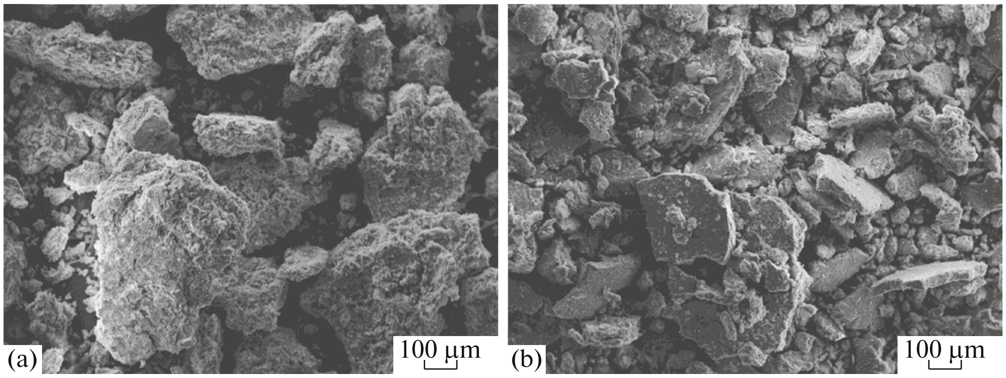

Fig. 2. SEM images: (a) potassium aluminosilicate, sample I; (b) sodium aluminosilicate, sample II.

determined for the Langmuir equation are shown in Table 1.

Estimates of the sorption kinetics of Cs^+ ions in the sorption time range of 1 to 60 min showed that the kinetic curve reached a plateau within the first 5 min, and the sorption value did not change subsequently (Fig. 4). The degree of Cs^+ ion extraction was 90.3% for sorbent I and to 96.9% for sorbent II as soon as 1 min later.

The apparent pseudo-high-speed constants k_1 and k_2 and the corresponding squares of correlation coefficients R^2, which corroborated a correct correlation to kinetic models of pseudo-first and pseudo-second orders, are shown in Table 2. We can see the sorption of Cs^+ ions by the investigated materials in the considered time range was described more accurately by the pseudo-second order model, as was indicated by the corresponding correlation coefficients.

Analysis of K^+ and Na^+ ions concentrations in the filtrates upon sorption showed that upon an increase in the concentration of Cs^+ ions in the solution, the concentration of K^+ ions rose from 2.0 to 17.3 mmol L^{-1} (in experiments with sorbent I), while that of Na^+ ions rose from 1.9 to 22.1 mmol L^{-1} (in experiments with sorbent II), relative to the reference sample. These data were corroborated by the results from elemental analysis of the solid residues after sorption, which showed an increase in the concentration of cesium in the samples and drop in the concentration of the corresponding alkaline metal. This means the sorption mechanism in the investigated materials was the cation exchange of K^+ and Na^+ ions by Cs^+ ions in the synthesized aluminosilicate sorbents.

CONCLUSIONS

Our synthesized samples of potassium and sodium aluminosilicates had ratios of Al : Si = 1 : 1.74 and 1 : 1.39, respectively, while their specific surface areas were 84.8 and 32.7 m^2/g, respectively. The materials were X-ray amorphous with partial crystallization of potassium aluminosilicate and the formation of $NaAlSiO_4$ phase after annealing at 1000°C. The sorption capacity of potassium aluminosilicate with respect to cesium

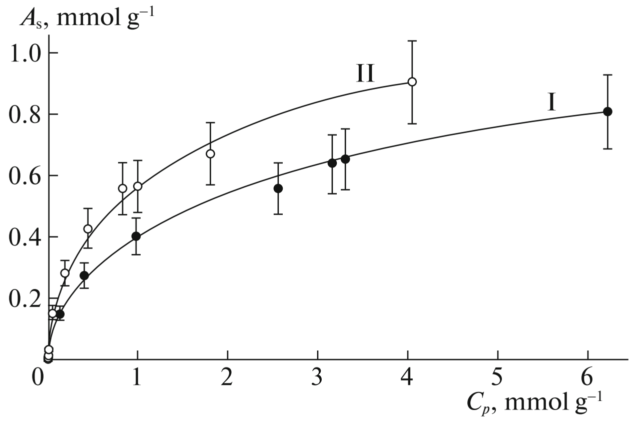

Fig. 3. Isotherms of the sorption of Cs^+ ions by samples I and II.

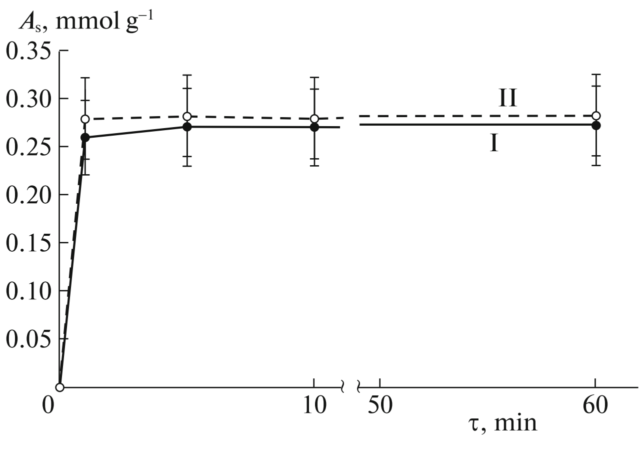

Fig. 4. Kinetic dependences of sorption of Cs^+ ions by (I) potassium and (II) sodium aluminosilicates.

Table 1. Parameters of the Langmuir equation upon sorption of Cs^+ ions by sorbents I and II

Sorbent	k, L mmol^{-1}	A_m, mmol g^{-1}	R^2
I	1.53	0.822	0.9682
II	2.61	0.93	0.9693

Table 2. Results from processing the kinetic curves of Cs^+ ion sorption by potassium (I) and sodium (II) aluminosilicates

Sample	Kinetic model			
	pseudo-first order		pseudo-second order	
	k_1, min^{-1}	R^2	k_2, g mmol^{-1} min^{-1}	R^2
I	0.096	0.6926	68.0	0.9999
II	0.025	0.6926	48.5	0.9999

ions was higher than that of sodium aluminosilicate, and the sorption isotherms obeyed the Langmuir equation. The kinetic curve reached a plateau within the first 5 min, and the sorption kinetics were described by a pseudo-second order model. Cesium ions were mainly sorbed according to a cation exchange mechanism.

ACKNOWLEDGMENTS

This work was supported by RF Presidential Grant for Young Scientists and Researchers no. MK-2884.2017.3. It was performed as part of a State Task for educational institutions from the RF Ministry of Science and Education, project no. 4.5913.2017/8.9.

REFERENCES

1. V. I. Sergienko, L. A. Zemnukhova, A. G. Egorov, et al., Ross. Khim. Zh. **68** (3), 116 (2004).
2. R. C. Sun, *Cereal Straw As a Resource for Sustainable Biomaterials and Biofuels* (Elsevier, Amsterdam, 2010).
3. A. G. Savinykh, B. A. Glazman, N. S. Nikolaeva, and N. I. Isaikina, Tr. VNIIgidroliz, No. 30, 36 (1980).
4. A. R. Staniforth, *Cereal Straw* (Oxford, 1979).
5. A. G. Ladatko, L. A. Zemnukhova, G. A. Fedorishcheva, and V. A. Kovalevskaya, Risovodstvo, No. 7, 100 (2005).
6. Yu. M. Nikolenko, A. N. Kholomeidik, L. A. Zemnukhova, et al., Vestn. DVO RAN, No. 5, 70 (2012).
7. L. A. Zemnukhova, O. D. Aref'eva, G. A. Fedorishcheva, and A. A. Kovshun, Ekol. Prom-st' Rossii, No. 2, 49 (2011).
8. L. A. Zemnukhova, O. D. Aref'eva, and A. A. Kovshun, Khim. Interesah Ustoich. Razvit. **19**, 509 (2011).
9. L. A. Zemnukhova, S. V. Tomshich, V. A. Mamontova, N. A. Komandrova, G. A. Fedorishcheva, and V. I. Sergienko, Russ. J. Appl. Chem. **77**, 1883 (2004).
10. G. P. Shchetinina, B. B. Chernov, L. A. Zemnukhova, and U. V. Kharchenko, Transp. Delo Ross., Spec. Iss. No. 3, 135 (2005).
11. L. A. Zemnukhova, L. G. Kolzunova, O. D. Aref'eva, et al., Voda: Khim. Ekol., No. 9, 86 (2014).
12. L. A. Zemnukhova, G. A. Fedorishcheva, E. A. Tsoi, and O. D. Aref'eva, RF Patent No. 2557607, Byull. Izobret., No. 21 (2015).
13. P. S. Gordienko, I. A. Shabalin, and S. B. Yarusova, RF Patent No. 2516639, Byull. Izobret., No. 14 (2014).
14. P. S. Gordienko, I. A. Shabalin, and S. B. Yarusova, RF Patent No. 2510292, Byull. Izobret., No. 9 (2014).
15. P. S. Gordienko, S. B. Yarusova, S. B. Bulanova, et al., Khim. Tekhnol. **14**, 185 (2013).
16. P. S. Gordienko, S. B. Yarusova, I. A. Shabalin, V. V. Zheleznov, N. V. Zarubina, and S. B. Bulanova, Radiochemistry **56**, 607 (2014).
17. W.-C. Tan, S.-Y. Yap, A. Matsumoto, et al., Adsorption **17**, 863 (2011).
18. P. Thuadaij and A. Nuntiya, Proc. Eng. **32**, 1026 (2012).
19. S. Bohra, D. Kundu, and M. K. Naskar, Ceram. Int. **40**, 1229 (2014).
20. R. M. Mohamed, I. A. Mkhalid, and M. A. Barakat, Arab. J. Chem. **8**, 48 (2015).
21. E.-P. Ng, H. Awala, K.-H. Tan, et al., Microporous Mesoporous Mater. **204** (2015).
22. I. O. Ali, M. S. Thabet, K. S. El-Nasser, et al., Microporous Mesoporous Mater. **160**, 97 (2012).
23. I. O. Ali, T. M. Salama, M. S. Thabet, et al., Mater. Chem. Phys. **140**, 81 (2013).
24. N. J. Coleman, D. S. Brassington, A. Raza, and A. P. Mendham, Waste Manage. **26**, 260 (2006).
25. Y. S. Ho and G. McKay, Process Biochem. **34**, 451 (1999).
26. I. I. Plyusnina, *Infrared Spectra of Minerals* (Mosk. Gos. Univ., Moscow, 1976) [in Russian].

Translated by D. Marinin